Gridding Techniques for the Level Set Method in Semiconductor Process and Device Simulation

Edwin C. Kan, Ze-Kai Hsiau, Vinay Rao and Robert W. Dutton
CISX 334, Stanford University, Stanford, CA 94305, USA

***Abstract*—Owing to the static and nonconformal mesh it employs, the level-set method for geometry representation offers several attractive alternatives for boundary movement and finite element schemes in comparison with conformal boundary representation. For boundary movement problems, the adaptive gridding schemes for the level-set method are analyzed for their applicability on tracing thin-film characteristics. For finite element schemes on non-interface-conformal mesh, advantages for additional trial functions based on the level-set function are illustrated by solving a partial differential equation on a geometry with rough interface.**

I. Introduction

The level-set method [1], [2] was originally proposed for tracing the curvature-dependent advancing front in crystal growth and flame propagation with numerical solutions of the Hamilton-Jacobi equation. The basic idea behind the level-set function is simple: instead of continuously updating the geometrical boundary of an advancing front, a level-set function, which is the signed distance to the closest boundary of the geometry, is updated for every time step on a stationary grid. It is also found to be very attractive for simulating thin-film growth and patterning in semiconductor manufacturing processes since conservation laws can be expressed rigorously without *ad hoc* delooping algorithm. However, solving the Hamilton-Jacobi equation everywhere with a homogeneous tensor-product grid is very expensive. There are two most popular adaptive gridding schemes for implementation of the level-set method, namely the thin-tube [1], [3] and the quad/oct tree algorithms [2], [3]. In this paper, it will be shown that the quad/oct tree algorithm is more appropriate for applications considering not only the moving boundary of the device geometry but also the distributive thin-film characteristics (such as residual stress and average grain size) during the processing steps. Moreover, since a completely valid volume grid is maintained for the active region to keep track of the geometry by the level-set function, the algorithm can also be applied to eliminate the constraint of gridding conformity to the material interface with special element trial functions to handle possible interface discontinuities [7], [8]. This is even useful for the case of static geometry gridding, since interface conformity often causes enormous amount of grid points for rough surfaces (if not divergence) due to Steiner-point propagation. Simulation of residual stress during oxide deposition and device simulation of a MOS capacitor with a rough interface will be used as examples for this gridding algorithm.

E. C. Kan, 415-723-9796, fax 415-725-7731, kan@gloworm.stanford.edu, http://www.stanford.edu/~kan.

This work was supported in part by DARPA under contracts DABT63-93-C-0053 and F30602-96-2-0308.

II. Trace of Thin-film Characteristics During Deposition and Etching

Modeling of thin-film characteristics such as impurity concentration and stress during material growth has become increasingly important for technology scaling and microelectro-mechanical system (MEMS) applications [5]. Traditionally the etching and deposition simulation is only used to characterize the final geometry [2], and the gridding algorithms are selected by only considering efficiency and accuracy for boundary movement, since the stress and density gradients in deposited material are usually relatively small and has minimal effects on its electrical properties. However, to achieved stacked active devices in VLSI, in-situ fabrication of p-n junctions during deposition is a promising process. Also, for MEMS, even with a considerably small residual stress, the final geometry and mechanical behavior will be significantly different. These distributive thin-film characteristics, obtained either from solving an additional equation or from analytical calculation, need to be recorded together with boundary movement of the geometry.

The level-set method for boundary movement with grid adaptivity by either thin-tube [1], [3] or quad/oct tree [2], [3] algorithms shows a good trade-off among accuracy, robustness and efficiency. The thin-tube algorithm calculates the level-set function based on a homogeneous tensor-product mesh, but only the mesh points close to the current moving front are used and stored. The time step is controlled so that no boundary will cross more than one element for both numerical stability and for thin-tube validity. On the other hand, the quad tree adaptivity is achieved by recursive refinements of elements with area A satisfying

$$A > |\bar{\phi}|^2 \text{ and } A > \text{MinimumAreaAllowed} \qquad (1)$$

where $\bar{\phi}$ is the average magnitude of the level set function. The thin-tube algorithm is estimated to be 2 to 3 times

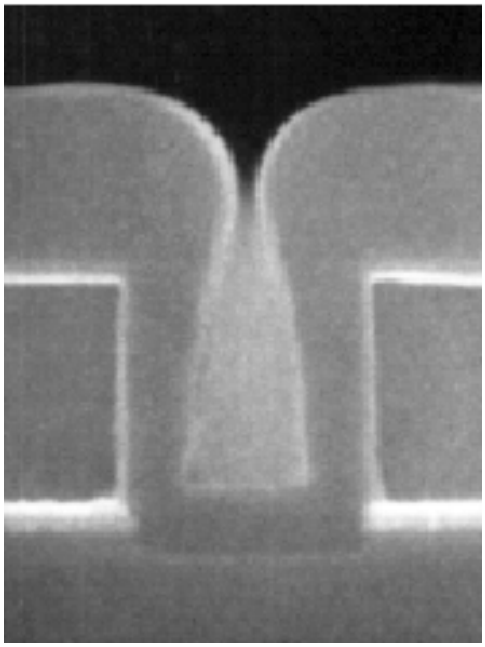

Fig. 1. SEM of LPCVD SiO_2 deposition for trench filling.

faster than the quad tree algorithm for the computational steps related to the level-set function updates.

However, if it is necessary to trace material characteristics together with boundary movement, the quad/oct tree algorithm is more appropriate by employing an additional refinement criterion to properly resolve the field gradients:

$$\nabla\varphi > \text{Threshold for } \nabla\varphi \tag{2}$$

where φ is the recording field-on-mesh. There is no known method for adaptively recording the field-on-mesh with the thin-tube algorithm. As an illustration, Fig. 1 shows the low-pressure chemical vapor deposition (LPCVD) of SiO_2 from silane. Since the gas transport is calculated by ray-tracing visibility and surface reaction is modeled by sticking coefficients, the computational time for updating the level-set function is a small fraction of the total execution time. Fig. 2 shows the simulated profile evolution by the software SPEEDIE [2], where the parameters in various gridding schemes are tuned to give similar accuracy on the final geometry. The processing temperature is 380°C. The viscosity of oxide can be ignored and the oxide can be modeled as an isotropic elastic solid. The hydrostatic part of the stress is calculated during the deposition simulation and the quad tree mesh adapts to the level-set function, the local curvature [4] and the stress gradients (Fig. 3). In comparison, the grid that only adapts to the level-set function is shown in Fig. 4. It is clear that the details of stress gradients will be lost in Fig. 4. There are 2,652 grid points in Fig. 3. In contrast, if the thin-tube algorithm is used and the resolution of stress gradients needs to be preserved, 16,384 grid points are necessary. The ratio of the number of grid points will be even larger for 3D cases.

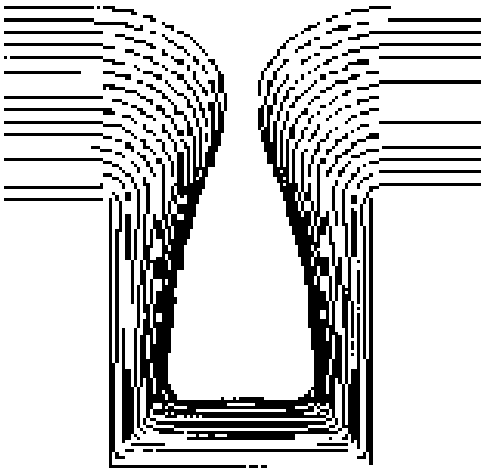

Fig. 2. Simulated profile evolution for Fig. 1.

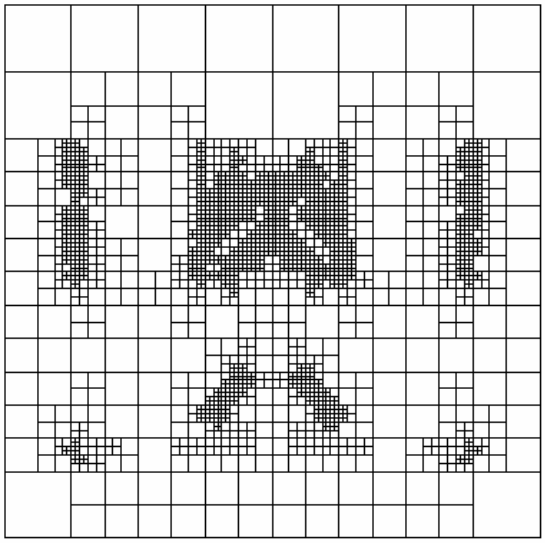

Fig. 3. The quad tree mesh adapted to the level-set function, local curvature and the stress gradient.

III. Elimination of Grid Conformity to Material Interface

For an abrupt material interface, the field variables (e.x., dopant concentration) and model coefficients (e.x., dielectric constant) used in a partial-differential-equation (PDE) system can be discontinuous across the material interface. Electric potential across an interface with surface trap or charge, dopant segregation in Si/SiO_2 interface and carrier concentration across a Schottky contact are all examples for such discontinuity. Gridding is often conformal to the interface for convenient treatment of the interface condition by either the finite difference or the finite element schemes. For planar interface in Manhattan-like geometry, the conformal constraint is usually easy to satisfy. However, for rough interfaces or complex geometries, especially in 3D cases, interface conformity may introduce an enormous number of grid points, or even failure of convergence with respect to grid quality constraints. To eliminate the conformal constraint, it

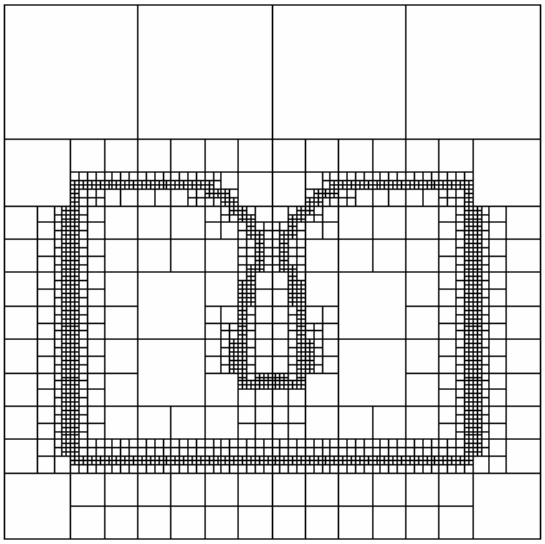

Fig. 4. The quad tree mesh adapted to the level set function only.

is proposed in this work to use the level-set function to describe the static rough interface, which is equivalent to an Eulerian representation with roughness features being nodal exact and smoothed by second-order polynomials within the elements containing the boundary. The usual linear roof-top trial functions for finite element schemes will give a poor approximation to the discontinuous fields within the element. Although various shock-tracking algorithms for finite element schemes are available using either grid or functional adaptivity[6], yet the origin of the discontinuity is very different from shocks generated from supersonic flow problems. The abrupt material interface causes the *jump*, whose position can be accurately determined by the level-set function and whose magnitude is govern by analytical interface conditions. Better capabilities to represent the discontinuity within the elements can be achieved by augmenting special trial functions [7], [8]. For discontinuous fields, an additional trial function is used to capture the jump condition. The trial function for a triangular element is illustrated in Fig. 5(a) with its mathematical form as

$$\frac{N_2(x,y)+N_3(x,y)}{N_2(\xi_0,\eta_0)+N_3(\xi_0,\eta_0)} - \frac{N_1(x,y)}{N_1(\xi_0,\eta_0)}\,, \qquad (3)$$

where N_1, N_2 and N_3 are the original roof-top trial functions (e.x., $N_1 = 1$ at node 1 and $N_1 = 0$ at nodes 2 and 3), and (ξ_0, η_0) denotes the center point of the jump determined by the level-set function on the nodes. For continuous fields with jumps in the derivatives caused by discontinuous material parameters, the trial function is of the form

$$\frac{N_2(x,y)+N_3(x,y)}{N_2(\xi_0,\eta_0)+N_3(\xi_0,\eta_0)} + \frac{N_1(x,y)}{N_1(\xi_0,\eta_0)}\,, \qquad (4)$$

which is illustrated in Fig. 5(b).

The advantages of this approach include simpler gridding and accurate estimations of the surface normal and curvature. There may be however some computational

Fig. 5. New trial functions for (a) discontinuous fields and (b) fields with discontinuous derivatives.

penalty, since the number of field variables (and corresponding PDEs) needs to be identical across the interface. The nonlinear Poisson equation for analyzing a MOS capacitor with a rough interface extracted from atomic force microscopy (AFM) [9] will be used to illustrate the new algorithm. The interface condition is described by

$$\epsilon_{si}\left.\frac{d\psi}{d\hat{n}}\right|_{si} - \epsilon_{ox}\left.\frac{d\psi}{d\hat{n}}\right|_{ox} = Q_{int} + Q_{itrap}(\psi) \qquad (5)$$

where ψ is the electrostatic potential, ϵ_{si} and ϵ_{ox} are the dielectric constants for silicon and oxide, Q_{int} and Q_{itrap} are the interface charge and trap concentration, and $\hat{n}$ is the surface normal. Notice that nonzero Q_{int} and Q_{itrap} will make the potential discontinuous and $\epsilon_{ox} \neq \epsilon_{si}$ will make the derivative of the potential discontinuous. The surface normal $\hat{n}$ needs to be accurately calculated for rough interface to maintain numerical consistency. For the magnitude of roughness shown, approximation of $\hat{n}$ by y may not be acceptable. Fig. 6 shows the grid conformal to the interface. To have a reasonable resolution of the rough interface, dense grids are required in the vicinity of the interface and the Steiner points for grid quality enhancement propagate far into the bulk region. Fig. 7 shows the grid with the level set function employing the additional trial function in Fig. 5. The grid is regular

and grid quality is guaranteed. The solutions of the Poisson equation for the test structure from both schemes are very close to each other and are shown shown in Fig. 8. For handling complex 3D structures, our approach may appear even more attractive.

IV. Conclusion

For applications beyond boundary movement, the gridding requirements for the level-set methods are carefully examined. For computing and recording nonhomogeneous field-on-mesh, quad/oct tree adaptive schemes are shown to be very effective. For treating discontinuous fields across abrupt material interface in finite element schemes, additional trial functions based on the level-set method can eliminate the interface-conformal constraints on gridding.

References

[1] D. Adalsteinsson and J.A. Sethian, "A fast level set method for propagating interfaces," *J. Comp. Phys.*, vol. 118, pp. 269-277, 1995.

[2] Z. Hsiau, E. C. Kan, J. P. McVittie and R. W. Dutton, "Physical etching/deposition simulation with collision-free boundary movement," *IEDM Tech. Dig.*, 1995, p. 101.

[3] B. Milne, *Ph.D. Thesis*, Dept. of Mathematics., UC Berkeley, 1995.

[4] Z. Hsiau, E. C. Kan, J. P. McVittie and R. W. Dutton, "2D/3D Etching and Deposition Simulation Tools Implemented with a General TCAD Geometry Server, " *Techcon Dig.*, 1996, Pheonix, AZ, Sept. 1996.

[5] P. A. Beck, S. M. Taylor, J. P. McVittie and S. T. Ahn, "Low Stress silicon nitride and polysilicon films for micromachining applications, " *Mat. Res. Soc. Symp. Proc.*, vol. 182, p. 207, 1990.

[6] T. J. R. Hughes, Prentice Hall, Englewood Cliffs, New Jersey, 1987.

[7] F. Armero and K. Garikipati, "An analysis of strong discontinuities in multiplicative finite strain plasticity and their relation with the numerical simulation of strain localization in solids, " *Intl. J. Solids and Structures*, vol. 33, no. 20-22, pp. 2863-85, 1996.

[8] V. S. Rao, T. J. R. Hughes, E. C. Kan and R. W. Dutton, "A new numerical formulation for thermal oxidation, " *Proc. SISPAD*, Boston, Sept. 1997.

[9] H. C. Lin, E. C. Kan, T. Yamanaka and C. R. Helms, *Proc. Symp. VLSI Technology*, Kyoto, Japan, June 1997.

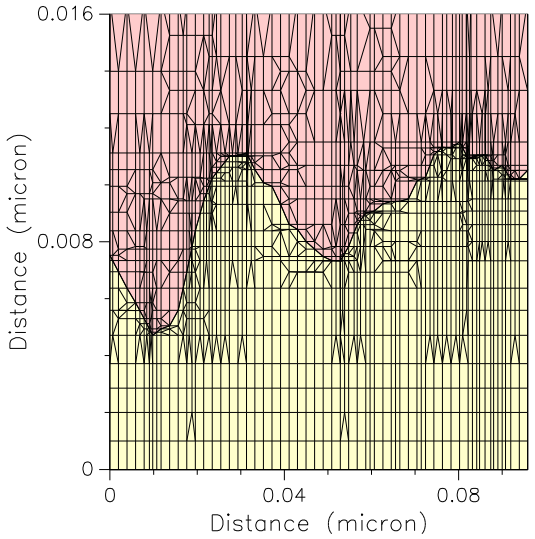

Fig. 6. Interface conformal grid for MOS capacitor with a rough surface.

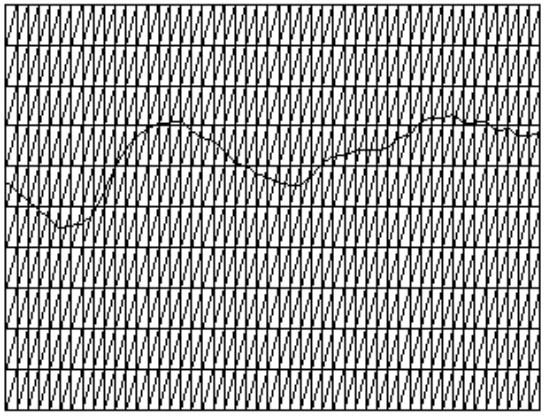

Fig. 7. Grid nonconformal to the rough interface using the discontinuous element technology.

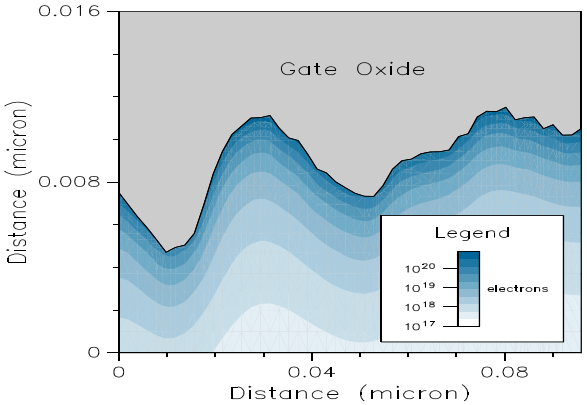

Fig. 8. The numerical solution for the MOS capacitor based on (1). The two gridding schemes give similar accuracy.